THE JOURNAL OF BIOLOGICAL CHEMISTRY VOL. 286, NO. 11, pp. 8846–8856, March 18, 2011
Printed in the U.S.A.

Lysyl Hydroxylase 3 Glucosylates Galactosylhydroxylysine Residues in Type I Collagen in Osteoblast Culture*

Received for publication, August 24, 2010, and in revised form, December 17, 2010 Published, JBC Papers in Press, January 10, 2011, DOI 10.1074/jbc.M110.178509

Marnisa Sricholpech[‡], Irina Perdivara[§], Hideaki Nagaoka[‡], Megumi Yokoyama[‡], Kenneth B. Tomer[§], and Mitsuo Yamauchi[‡1]

From the [‡]North Carolina Oral Health Institute, School of Dentistry, University of North Carolina, Chapel Hill, North Carolina 27599 and [§]Laboratory of Structural Biology, NIEHS, National Institutes of Health, Research Triangle Park, North Carolina 27709

Lysyl hydroxylase 3 (LH3), encoded by *Plod3*, is the multifunctional collagen-modifying enzyme possessing LH, hydroxylysine galactosyltransferase (GT), and galactosylhydroxylysine-glucosyltransferase (GGT) activities. Although an alteration in type I collagen glycosylation has been implicated in several osteogenic disorders, the role of LH3 in bone physiology has never been investigated. To elucidate the function of LH3 in bone type I collagen modifications, we used a short hairpin RNA technology in a mouse osteoblastic cell line, MC3T3-E1; generated single cell-derived clones stably suppressing LH3 (short hairpin (Sh) clones); and characterized the phenotype. *Plod3* expression and the LH3 protein levels in the Sh clones were significantly suppressed when compared with the controls, MC3T3-E1, and the clone transfected with an empty vector. In comparison with controls, type I collagen synthesized by Sh clones (Sh collagen) showed a significant decrease in the extent of glucosylgalactosylhydroxylysine with a concomitant increase of galactosylhydroxylysine, whereas the total number of hydroxylysine residues was essentially unchanged. In an *in vitro* fibrillogenesis assay, Sh collagen showed accelerated fibrillogenesis compared with the controls. In addition, when recombinant LH3-V5/His protein was generated in 293 cells and subjected to GGT/GT activity assay, it showed GGT but not GT activity against denatured type I collagen. The results from this study clearly indicate that the major function of LH3 in osteoblasts is to glucosylate galactosylhydroxylysine residues in type I collagen and that an impairment of this LH3 function significantly affects type I collagen fibrillogenesis.

Collagens are a large family of extracellular matrix proteins comprising at least 29 different genetic types (1, 2). Among those types, fibrillar type I collagen is the most abundant protein, and it is the major structural component in most connective tissues, including bone. One of the critical steps in collagen biosynthesis, which contributes to the functional integrity of the tissues, is the post-translational modifications, including the hydroxylation of specific proline (Pro) and lysine (Lys) residues, glycosylation of specific hydroxylysine (Hyl)[2] residues, and the formation of covalent intermolecular cross-links. Although several functions have been proposed for collagen glycosylation, such as control of collagen fibrillogenesis (3–7), cross-linking (8–14), remodeling (15–22), and collagen-cell interaction (23, 24), the function is still not well defined due in part to the lack of clear understanding in the mechanism of this modification.

In fibrillar collagens, glycosylation occurs at specific Hyl residues by hydroxylysine galactosyltransferase (GT) (EC 2.4.1.50) and galactosylhydroxylysine-glucosyltransferase (GGT) (EC 2.4.1.66) resulting in the formation of galactosylhydroxylysine (G-Hyl) and glucosylgalactosylhydroxylysine (GG-Hyl), respectively. Recently, these enzymatic activities were found in the multifunctional enzyme lysyl hydroxylase 3 (LH3), one of the collagen-modifying enzymes in the LH family, encoded by *Plod3* (25–27).

The GT and GGT activities of LH3 were identified by measuring the transfer of radiolabeled sugar moieties to Hyl residues in calf skin gelatin substrate (25, 27). The biological significance of the GGT activity of LH3 in the biosynthesis of collagen types IV and VI has been demonstrated from the studies of LH3-deficient mice (28–30). In addition, defective GGT activity resulting from four polymorphic nucleotides in the non-coding region of *Plod3* was detected in a family with dominant epidermolysis bullosa simplex (31, 32). In another recent finding, two heterozygous mutations in the *Plod3* coding region have been associated with a rare syndrome of congenital malformations affecting several connective tissues and organs (33). As for the GT activity of LH3, the data have been somewhat conflicting, and the biological significance is still not clearly understood. This activity could be performed by recently reported novel enzymes, glycosyltransferase 25 domains 1 and 2 encoded by *GLT25D1* and *GLT25D2*, respectively (34).

It has been reported that altered collagen glycosylation is associated with bone disorders (35–42). However, the role of LH3 in type I collagen modification and bone biology has not been investigated.

To elucidate the function of LH3 for bone type I collagen, we used an *in vitro* loss-of-function approach in a mouse osteo-

* This work was supported, in whole or in part, by National Institutes of Health Grants R21DE019569 and R01 DE10489 and Intramural Research Program NIEHS Project ES050171.

[1] To whom correspondence should be addressed: CB 7454, NC Oral Health Inst., University of North Carolina, Chapel Hill, NC 27599. Tel.: 919-425-3570; Fax: 919-425-3535; E-mail: mitsuo_yamauchi@dentistry.unc.edu.

[2] The abbreviations used are: Hyl, hydroxylysine; G-Hyl, galactosylhydroxylysine; GG-Hyl, glucosylgalactosylhydroxylysine; LH, lysyl hydroxylase; GT, hydroxylysine galactosyltransferase; GGT, galactosylhydroxylysine-glucosyltransferase; MC, MC3T3-E1; EV, empty vector; Bis-Tris, 2-[bis(2-hydroxyethyl)amino]-2-(hydroxymethyl)propane-1,3-diol; CBB, Coomassie Brilliant Blue.

blast-like cell line, MC3T3-E1 (MC), by generating single cell-derived clones stably suppressing LH3. Type I collagen produced by the clones was analyzed for the extent of modifications (*e.g.* GG-Hyl, G-Hyl, and free Hyl) and fibrillogenesis. In addition, recombinant LH3-V5/His fusion protein was generated, and its enzymatic functions were investigated by means of a newly developed high performance liquid chromatography (HPLC)-based glycosyltransferase activity assay.

EXPERIMENTAL PROCEDURES

Cell Lines and Culture Conditions—MC subclone 4, a well characterized nontransformed mouse osteoblast-like cell line (43), was purchased from American Type Culture Collection (CRL-2593). The cells were grown in α-minimum essential media (Invitrogen) containing 10% FBS (Invitrogen) and supplemented with 100 units/ml penicillin G sodium and 100 μg/ml streptomycin sulfate. 293 human embryonic kidney (HEK) cells were purchased from Clontech. The cells were maintained in Dulbecco's modified Eagle's medium (DMEM; Invitrogen) with high glucose (4.5 g/liter) and the same supplements as described above. Both cell lines were cultured in a 5% CO_2 atmosphere at 37 °C, and the medium was changed twice a week.

Expression of Plod Family, Glt25d1, and Glt25d2 in MC Cells—MC cells were plated at a density of 2×10^5 cells/35-mm dish; after 48 h, total RNA was extracted with TRIzol reagent (Invitrogen); and 2 μg of total RNA was converted into cDNA by using the Omniscript reverse transcriptase kit (Qiagen, Valencia, CA). Quantitative real time PCR was performed using the sequence-specific primers for LH1 (*Plod1*; Applied Biosystems assay number Mm00599925_m1), LH2 (*Plod2*; Mm00478767_m1), LH3 (*Plod3*; Mm00478798_m1), Glt25d1 (*Glt25d1*; Mm00600638_m1), and Glt25d2 (*Glt25d2*; Mm00625070_m1). The reactions were prepared and analyzed in triplicates by the ABI Prism 7000 Sequence detection system (Applied Biosystems, Foster city, CA). The mRNA expression level of LH3 relative to glyceraldehyde-3-phosphate dehydrogenase (GAPDH; Applied Biosystems assay number 4308313) was analyzed by the $2^{-\Delta\Delta CT}$ method (44).

Generation of Short Hairpin-expressing Plasmid Targeting Plod3—The target sequences for suppression of *Plod3* were designed using the siDesign Center web site (Dharmacon RNAi Technologies). The three highest ranked targets were selected (si1, AGAAGGAAATGGAGAAATA (start position 956); si2, CCACAAGGGTGTAGATTAT (2715); and si3, GAACAAAACAGGAAGGTAA (1897)) and converted into short hairpin oligonucleotide sequences specific for pSilencer2.1 vector by the siRNA converter (Ambion, Austin, TX). This method added BamHI and HindIII restriction site overhangs at the 5′-end of the sense and antisense oligonucleotide, respectively, to facilitate efficient directional cloning into the pSilencer vectors. The two complimentary 55-mer oligonucleotides for each target were ordered (Eurofins MWG Operon, Huntsville, AL) and annealed in the annealing buffer (10 mM Tris, pH 7.5–8.0, 50mM NaCl, 1 mM EDTA) according to the condition described in the instruction manual for pSilencer2.1 vector. The annealed oligonucleotides were then ligated into the pSilencer2.1-U6/neo vector (Ambion), linearized with BamHI and HindIII restriction enzyme digestion, and transformed into bacterial competent cells. The clones with 100% nucleotide sequence accuracy (Eton Bioscience, Durham, NC) for each target (Sh1, Sh2, and Sh3) were selected and tested for their suppression efficiency by transient transfection into MC cells using FuGENE 6 transfection reagent (Roche Applied Science). The non-transfected MC cells and those transfected with the original pSilencer2.1-U6/neo plasmid (empty vector (EV); encoding a hairpin siRNA sequence not found in any genome database) were used as controls. After 48 h, total RNA was extracted, converted into cDNA, and analyzed for the expression of *Plod3* by quantitative real time PCR as described above. The suppression efficiency among the different shRNA target sites was then compared (in percent) relative to the controls.

Generation and Characterization of MC Single Cell-derived Clones Stably Suppressing LH3—MC cells were transfected with the selected pSilencer2.1-U6/neo-Plod3 plasmid by using FuGENE 6 transfection reagent (Roche Applied Science). After 48 h, the transfected cells were trypsinized, plated at a low density, and maintained under constant selection with 400 μg/ml G418 sulfate (Mediatech, Inc., Manassas, VA). Several single cell-derived short hairpin (Sh) clones were isolated by cloning rings and maintained in α-minimum essential medium, 10% FBS, 100 units/ml penicillin, 100 μg/ml streptomycin, and 400 μg/ml G418 sulfate. The single cell-derived EV clones were isolated and maintained in the same manner as described above. The selected Sh clones were then characterized by comparing the level of *Plod3* expression with those of the EV clone and the non-transfected MC cells by using quantitative real time PCR. Three to six Sh clones with different levels of *Plod3* suppression were then characterized for its effects on the mRNA expression of LH1 (*Plod1*; ABI assay number Mm00599925_m1), LH2 (*Plod2*; Mm00478767_m1), Glt25d1 (*Glt25d1*; Mm00600638_m1), and type I collagen α2 chain (*Col1A2*; Mm00483888_m1). The effect on cell proliferation was assessed by using the CellTiter 96 3-(4,5-dimethylthiazol-2-yl)-5-(3-carboxymethoxyphenyl)-2-(4-sulfophenyl)-2*H*-tetrazolium assay (Promega, Madison, WI) as reported previously (45).

Generation of Anti-mouse LH3 Antibody—Polyclonal rabbit anti-mouse LH3 antibody was commercially generated (Bethyl Laboratories, Inc., Montgomery, TX) by immunization with the HPLC-purified, synthetic peptide corresponding to amino acids 357–371 (FSAVKLVGPEEALSA) conjugated to keyhole limpet hemocyanin. The agarose-bound peptide was used for the affinity purification of the antibody from the hyperimmune rabbit serum obtained from the immunized animal. The sensitivity and specificity of the antibody was determined by Western blot analysis of purified recombinant LH3-V5/His-tagged protein as described below.

Immunoprecipitation and Western Blot Analysis—To determine the LH3 protein level, the Sh clones and the controls were plated onto 35-mm dishes at a density of 3×10^5 cells/dish. After culturing for 7days, the culture medium was collected; the cells were washed with PBS, lysed with lysis buffer (150 mM NaCl, 20 mM Tris-HCl, pH 7.5, 10 mM EDTA, 1% Triton X-100, 1% deoxycholate, 1.5% aprotinin, and 1 mM phenylmethylsulfonyl fluoride), and centrifuged; and the supernatant was col-

lected. The culture medium was incubated overnight with anti-LH3 antibody (see above) followed by incubation with protein G-Sepharose 4B-conjugated beads (Invitrogen) for 30 min, washed with lysis buffer, solubilized in SDS sample buffer (100 mM Tris-HCl, pH 8.8, 0.01% bromphenol blue, 36% glycerol, 4% SDS) in the presence of 10 mM dithiothreitol, and separated by a 4–12% NuPAGE Bis-Tris gel (Invitrogen). As for the cell lysates, the total protein concentration was measured by the DC protein assay kit (Bio-Rad) according to the manufacturer's protocol, and 20 μg of total protein was directly applied to a 4–12% NuPAGE Bis-Tris gel. The separated proteins were transferred to a polyvinylidene fluoride (PVDF) membrane (Immobilon-P, Millipore Corp., Bedford, MA) and subjected to Western blot analysis with anti-LH3 antibody followed by incubation with anti-rabbit IgG conjugated to alkaline phosphatase secondary antibody (Thermo Scientific, Rockford, IL). The immunoreactivities were detected with alkaline phosphatase conjugate substrate kit (Bio-Rad). Equal protein loading of cell lysate was confirmed by Western blotting with anti-β-actin antibody.

Purification of Type I Collagen—The same number of cells of MC, EV, and Sh clones were plated onto 10-cm dishes and maintained with twice-a-week change of medium (α-minimum essential medium, 10% FBS, 100 units/ml penicillin, 100 μg/ml streptomycin). When the cells reached confluence, 50 μg/ml ascorbic acid was added and cultured for at least 2 weeks, and then the cell/matrix layer was collected and subjected to type I collagen extraction as described previously (46). Briefly, the cells/matrices were washed with PBS and cold distilled water, lyophilized, and subjected to limited pepsin digestion (20%, w/w) in 0.5 N cold acetic acid with constant stirring at 4 °C for 24 h. After ultracentrifugation at 35,000 rpm for 2 h, the supernatant was collected, and type I collagen was precipitated with 0.7 M NaCl. The precipitate was then reconstituted with 0.5 N acetic acid, dialyzed against cold distilled water for 48 h at 4 °C, and lyophilized. Collagen solution was prepared by reconstituting the lyophilized collagen in 0.01 N acetic acid to a concentration of 0.5 μg/μl. The purity of type I collagen obtained from the control cells and clones was assessed by 6% Tris-glycine gel electrophoresis (Invitrogen) and staining with Coomassie Brilliant Blue (CBB) and by amino acid analysis (see below).

In Vitro Fibrillogenesis Assay—The procedure described previously (47) was slightly modified for the use of a 96-well microtiter plate. Briefly, lyophilized type I collagen purified from each group was redissolved in 0.01 M acetic acid at a concentration of 0.2 μg/μl. The reactions were prepared in triplicates in a 96-well microtiter plate (precooled on ice) containing the reaction buffer (140 mM NaCl, 30 mM sodium phosphate (PBS) at pH 7.3) (48) and purified type I collagen in a ratio of 1:1 (v/v) and placed in a Powerwave X 340 spectrophotometer (BioTek, Winooski, VT) equilibrated at 37 °C. Formation of collagen fibrils was monitored by measuring the absorbance at 400 nm (turbidity) at 1000-s intervals for 15 readouts. The turbidity-time curve was plotted, and the differences in the rate of collagen fibril formation and the potential fibril diameter among the clones and the controls were compared.

Purification of GG-Hyl and G-Hyl Standards—Natural marine sponge was used to isolate GG-Hyl residues (49, 50). Fifty milligrams of sponge was pulverized in a Spex freezer mill (SPEX CertiPrep, Metuchen, NJ), subjected to base hydrolysis with 2 N NaOH in sealed polypropylene tubes flushed with N_2 gas, and incubated at 110 °C for 22 h. The hydrolysate was acidified to ~pH 3 with 2 N HCl and filtered. It was then applied to a standardized molecular sieve column filled with Bio-Gel® P-2 resin (Bio-Rad) equilibrated in 0.1 N acetic acid buffer at a flow rate of 0.7 ml/min and monitored by absorbance at 214 nm (51). Several collagen cross-link standards were used as molecular weight standards to isolate the GG-Hyl (molecular mass, 487 Da)-enriched fractions. The GG-Hyl residues eluted slightly earlier than the pyridinoline standard (molecular mass, 428 Da). To generate the monoglycosylated form, G-Hyl, the purified GG-Hyl was subjected to mild acid hydrolysis with 0.8 N HCl at 110 °C for 1 h. The resulting G-Hyl was purified using the P-2 column as described above. The identities of the purified GG-Hyl and G-Hyl were confirmed by mass spectrometry.

Mass Spectrometry Analysis of Glycosylated Hydroxylysine Standards—The fraction containing GG-Hyl, G-Hyl, and free Hyl from the mild acid hydrolysis was analyzed by nanoelectrospray ionization-MS on a Waters QTof Global mass spectrometer (Milford, MA). A 1:100 dilution (v/v) in a solvent mixture containing 50% methanol in deionized water acidified with 0.1% formic acid was used for flow injection analysis. The mass spectra were acquired over the mass range m/z 150–1000. The source parameters used were as follows: capillary voltage, 3.5 kV; cone voltage, 80 V; collision energy, 10 V. The MS/MS spectra were acquired using targeted analysis of the ions of interest. The collision energy was optimized for each ion, ranging from 10 to 15 V for the singly protonated ion of G-Hyl and from 15 to 25 V for the singly protonated ion of GG-Hyl.

Quantification of GG-Hyl, G-Hyl, and Free Hyl—Lyophilized collagen samples were hydrolyzed with 6 N HCl (Sequenal grade; Thermo Scientific) *in vacuo* after flushing with N_2 at 110 °C for 22 h. The hydrolysates were subjected to amino acid analysis on a Varian 9050 HPLC system (9050/9012; Varian Associates Inc., Palo Alto, CA) equipped with a strong cation exchange column (AMINOSep catalog number AA-911, Transgenomic, Omaha, NE) (46). The level of total Hyl (GG-, G-, and free Hyl) in a collagen molecule was calculated based on the value of 300 residues of Hyp per collagen molecule.

To determine the level of glycosylated Hyl, lyophilized collagen samples were also subjected to base hydrolysis, and the hydrolysates were prepared in the same manner as described above. Then the GG-Hyl, G-Hyl, and free Hyl in the hydrolysates were separated and quantified with a specific gradient program (see Table 1) developed on the same HPLC system mentioned above. Separation of the different Hyl species from one another and from other amino acids was achieved in 75 min. The color factor of Hyl was used to calculate the quantity of GG-Hyl and G-Hyl (52–54). Because Hyp is partially degraded during base hydrolysis, the amount of total Hyl/collagen was determined by acid hydrolysis (see above). Based on the ratio of the three Hyl forms (GG-, G-, and free Hyl) and the total Hyl values obtained from acid hydrolysis, each form of Hyl was quantified as residues/collagen molecule.

Molecular Cloning of Mouse LH3 cDNA—Total RNA was isolated from MC cells using TRIzol reagent (Invitrogen)

according to the manufacturer's protocol. The first strand cDNA was synthesized from 2 μg of total RNA by means of the Omniscript reverse transcriptase kit (Qiagen). Specific primers for the coding sequence of mouse LH3 (GenBank™ accession NM011962) were designed as follows: forward primer, including restriction enzyme sequence for EcoRI, 5′-GCGAATTC-CGGGCCTGGGTGTAGCCT-′3; reverse primer, including the sequence for XhoI, 5′-GCCTCGAGGGGGTCAACAA-AGGACACCATG-′3. PCR amplification was performed by the ProofStart DNA polymerase (Qiagen) with an annealing temperature of 60.0 °C for 40 cycles. After digesting the PCR products with EcoRI and XhoI restriction enzymes, the inserts were ligated into the pcDNA3.1/V5-His-TOPO_verA vector (Invitrogen) generating the pcDNA3.1/LH3/V5-His constructs. The orientation and molecular size of the ligated insert of 2389 bp were analyzed by EcoRI and XhoI restriction enzyme digestion followed by 2% agarose gel electrophoresis. Plasmids containing digested inserts were sequenced at the University of North Carolina at Chapel Hill DNA Sequencing Facility and showed 100% homology to the mouse LH3 in the database.

Purification of LH3-V5/His Fusion Protein—293 HEK cells were transfected with pcDNA3.1/LH3/V5/His vector using FuGENE 6 transfection reagent (Roche Applied Science) according to the manufacturer's instructions, and the cells were cultured in the presence of 400 μg/ml G418 sulfate (Mediatech, Inc.) to isolate stably transfected single cell-derived clones. Based on Western blot analysis with anti-V5-alkaline phosphatase antibody, the clone that synthesized the highest level of LH3-V5/His protein was selected and cultured to collect the culture medium. LH3-V5/His protein was purified using a nickel-nitrilotriacetic acid-agarose resin (Qiagen) and eluted with elution buffer containing 0.2 M NaCl, 0.1 M glycine, 0.1% glycerol, 50 mM urea, 20 mM Tris, and 0.05 M histidine, pH 7.5. The purified proteins were pooled, dialyzed, concentrated with centrifugal filter with molecular weight cutoff 30,000 (Centricon, Millipore Corp.), and stored at −20 °C until use. The protein concentration was measured using a DC protein assay kit (Bio-Rad), and the purity of the purified LH3-V5/His protein was determined by a 4–12% NuPAGE Bis-Tris gel and CBB staining. To confirm its identity, the gel-resolved proteins were transferred to a PVDF membrane (Immobilon-P, Millipore Corp.) and subjected to Western blot analysis with anti-V5-alkaline phosphatase antibody (Invitrogen) or anti-LH3 antibody (Bethyl Laboratories, Inc.). The identity of the LH3-V5/His protein band and the specificity of the anti-LH3 antibody were confirmed by an immunizing peptide blocking experiment. Anti-LH3 antibody was preincubated with a 15, 30, or 60-fold molar excess of the blocking peptide (CFSAVKLVG-PEEALSA) for 30 min prior to immunoblotting. The immunoreactivities were detected as described above.

HPLC-based Collagen Glycosyltransferase Assays—Pepsinized bovine skin collagen solution (PureCol®, 3 mg/ml) was purchased from Advanced BioMatrix (Tucson, AZ). Denatured collagen substrate was prepared by incubating the PureCol solution in distilled water at 60 °C for 30 min and rapidly cooled on ice before use. The PureCol solution without heat denaturation was used as a native collagen substrate. The assay for GT or GGT reaction was performed in precooled 0.65-ml microcentrifuge tubes containing 120 μg of native or denatured collagen substrate, 60 μM UDP-Glc or UDP-Gal (Calbiochem/EMD Chemicals, Gibbstown, NJ), 12 μl of reaction buffer (16.7 mM MnCl2, 1 mM DTT, 2 mg/ml BSA, 0.1 M sodium bicarbonate buffer, pH 7.8), recombinant LH3-V5/His protein (1% (w/w) of collagen substrate), and distilled water in a total volume of 100 μl. The tubes were incubated at 37 °C for 45 min, and the reactions were terminated by placing the tubes on ice. The dose effects of recombinant LH3-V5/His protein on GT and GGT activities were evaluated using three concentrations of the protein, *i.e.* 1, 3, and 5% (w/w of collagen substrate). The reaction products were dried by speed vacuum centrifugation (Savant Instrument Inc., Hicksville, NY), hydrolyzed with base, and analyzed for the level of GG-Hyl, G-Hyl, and free Hyl as described above.

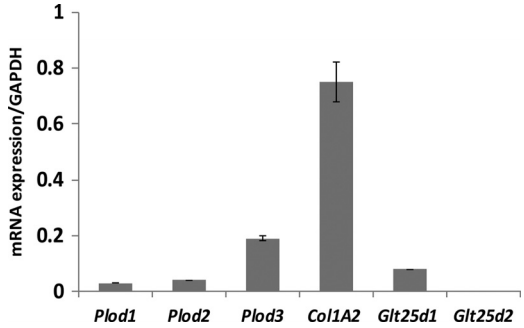

FIGURE 1. **Gene expression of *Plod* and *Glt25* families in MC cells.** After 48 h of culture of MC cells, the mRNA expression of *Plod1*, *Plod2*, *Plod3*, *Glt25d1*, and *Glt25d2* relative to internal control (GAPDH) was analyzed by quantitative real time PCR. Note that the expression of *Plod3* is the highest among all the genes, and only *Glt25d1*, but not *Glt25d2*, is expressed in MC cells. *Error bars* indicate mean ± S.D. of three independent experiments.

Statistical Analyses—Statistical analyses were performed using Jmp®8.0 software (SAS Institute Inc., Cary, NC). Statistical differences were determined by Kruskal-Wallis one-way analysis of variance and mean comparison with the controls by Dunnett's method. The data were presented as means ± S.D., and a p value less than 0.05 was considered significant.

RESULTS

Expression of Plod Family, Glt25d1, and Glt25d2 in MC Cells—At 48 h of MC cell culture, the expressions of *Plod1–3* and *Glt25d1–2* were analyzed by quantitative real time PCR. By normalizing to GAPDH, the results showed that *Plod3* was expressed at the highest level among the *Plod* family. In addition, *Glt25d1* was highly expressed in MC cells, whereas *Glt25d2* was undetectable (Fig. 1). The expression of *Plod3* and *Glt25d1* remained high, and that of Glt25d2 was undetectable up to 4 weeks of culture (data not shown). Among these genes, the highest expression was consistently observed for *Plod3*.

Generation of Clones Stably Suppressing Plod3—By transiently transfecting MC cells with pSilencer2.1-U6/Neo plasmids encoding hairpin oligonucleotides targeting three different sites in *Plod3*, the expression levels of *Plod3* relative to GAPDH from all three targets were significantly suppressed. In comparison with the non-transfected MC cells (100%), the expression levels of *Plod3* in Sh1, Sh2, and Sh3 were 20, 22, and 46%, respectively. The *Plod3* expression in the transfected control (EV) was ~80% of that of MC cells. The suppression levels

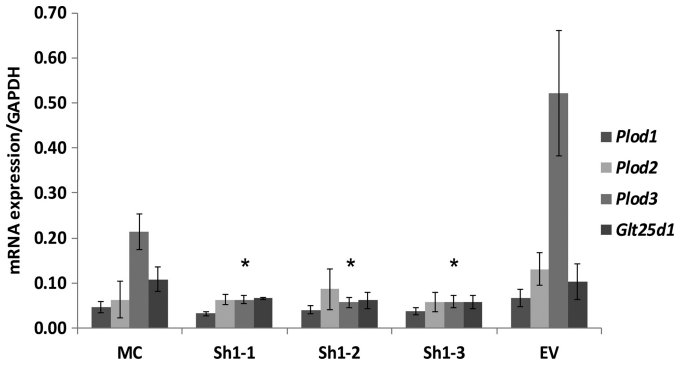

FIGURE 2. **Gene expression of *Plod* family and *Glt25d1* in single cell-derived Sh clones.** After 48 h of culture, real time PCR was performed to determine the suppression levels of *Plod3* in the single cell-derived Sh clones and its potential effects on *Plod1*, *Plod2*, and *Glt25d1* expression. The mRNA expression was normalized to the internal control (GAPDH). *Error bars* indicate mean ± S.D. of three independent experiments. *, significantly different ($p < 0.0001$) from MC and EV.

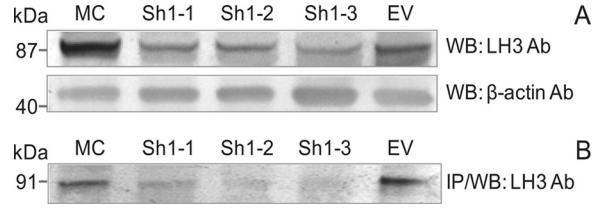

FIGURE 3. **Levels of LH3 protein produced by Sh1-derived clones and controls.** *A*, Western blot analyses of cell lysates with anti-LH3 antibody and anti-β-actin antibody. Twenty micrograms of total protein from each sample was loaded. *B*, immunoprecipitation-Western blot analyses of the culture media with anti-LH3 antibody. The intensity of the immunoreactive bands from Sh1-1, -2, and -3 was significantly lower than that of the controls, MC, and EV in both cell lysate and culture media. *WB*, Western blotting; *IP*, immunoprecipitation; *Ab*, antibody.

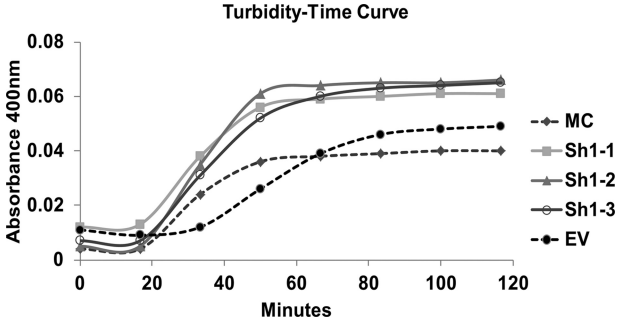

FIGURE 4. ***In vitro* fibrillogenesis assay.** After 2 weeks of culture, type I collagen without telopeptides was purified from the cell/matrix layers of MC cell, Sh (1-1, 1-2, and 1-3), and EV clones. Twenty micrograms of purified collagens (0.2 μg/μl) was incubated in a 96-well microtiter plate at 37 °C, and the 400-nm absorbance (turbidity) was measured (see "Experimental Procedures" for details). The kinetics of the collagen fibrils formation are shown as a turbidity-time plot.

of *Plod3* among the different targeting sequences were essentially the same when normalized to *Col1A2* (data not shown). Targeting sequence 1 (Sh1), showing the most suppression, was selected to generate single cell-derived clones stably suppressing LH3 by constant selection with G418 sulfate. Several clones were isolated and characterized.

Characterization of Sh1-derived Clones Stably Suppressing LH3—Three representative clones (Sh1-1, -2, and -3) stably suppressing *Plod3* that exhibited cell proliferation patterns similar to that of controls were selected for further characterization. Quantitative real time PCR analyses from three independent experiments showed statistically significant decreases in the expression of *Plod3* in all Sh clones ($p < 0.0001$) compared with the EV and MC controls (Fig. 2). The higher expression of *Plod3* in the EV clone compared with the MC parental cell was consistently observed during the isolation and characterization of the EV clones, likely due to the effect of transfection. The effect of *Plod3* suppression on the expression of the other *Plod* family members and *Glt25d1* was also investigated. When normalized to GAPDH, the expressions of *Plod2* and *Glt25d1* were not significantly changed in all three Sh clones when compared with the controls. *Plod1* expression was also mostly unaffected except for Sh1-1 in that the expression of *Plod1* was slightly lower when compared with EV ($p < 0.05$) but not significantly different from that in MC.

The LH3 protein levels from the clones were assessed by direct Western blot analysis for the cell lysate and immunoprecipitation/Western blot analysis for the culture medium (Fig. 3). In Fig. 3*A*, an immunoreactive band was observed at the expected molecular mass of LH3 at ~87 kDa in the cell lysates of the controls and the Sh clones; however, the intensity was decreased in all Sh clones. Comparable loading amounts of the cell lysates were confirmed by Western blotting detection of β-actin. Fig. 3*B* shows the result of immunoprecipitation followed by Western blot analysis with anti-LH3 antibody from the culture media collected from the clones and controls. Compared with the controls, all three Sh clones showed lower intensity of the immunoreactive bands observed at ~91 kDa. The apparent molecular mass of these bands was slightly higher than those observed in the cell lysate (~87 kDa). This observation is consistent with a previous report showing that the extracellular LH3 protein is modified by asparagine-linked glycosylation during the secretion process (55). Together, these data show that suppression of *Plod3* by short hairpin RNA expression plasmid resulted in decreases in the levels of LH3 protein both intra- and extracellularly.

Fibril Formation Kinetics of Purified Type I Collagen—Type I collagen without telopeptides was purified from the 2-week cell/matrix layer of the MC, EV, and Sh1-1, -2, and -3. The purity of the collagens was determined by 6% Tri-glycine gel electrophoresis where only the collagen-associated chains (α chains with some β and γ components) were identified (data not shown). In addition, amino acid analyses showed ~100 Hyp residues and ~340 glycine residues/1000 amino acids in MC, EV, and all the Sh clones, indicating a high level of collagen purity. The purified collagen from the clones and controls was subjected to an *in vitro* collagen fibrillogenesis assay to compare the fibril formation kinetics among the groups. Fig. 4 shows the turbidity-time curve plotted from the 400-nm absorbance measured over time. Compared with the controls, MC, and EV, the collagen from all three Sh clones showed a shorter lag time and higher turbidity plateau, indicating a faster rate of fibril formation and potentially larger collagen fibril diameter, respectively (56).

Purification and Nanoelectrospray Ionization-Quadrupole TOF Analysis of GG-Hyl and G-Hyl Standards—The GG-Hyl and G-Hyl residues were purified from the base hydrolysate of natural marine sponge by molecular sieve chromatography.

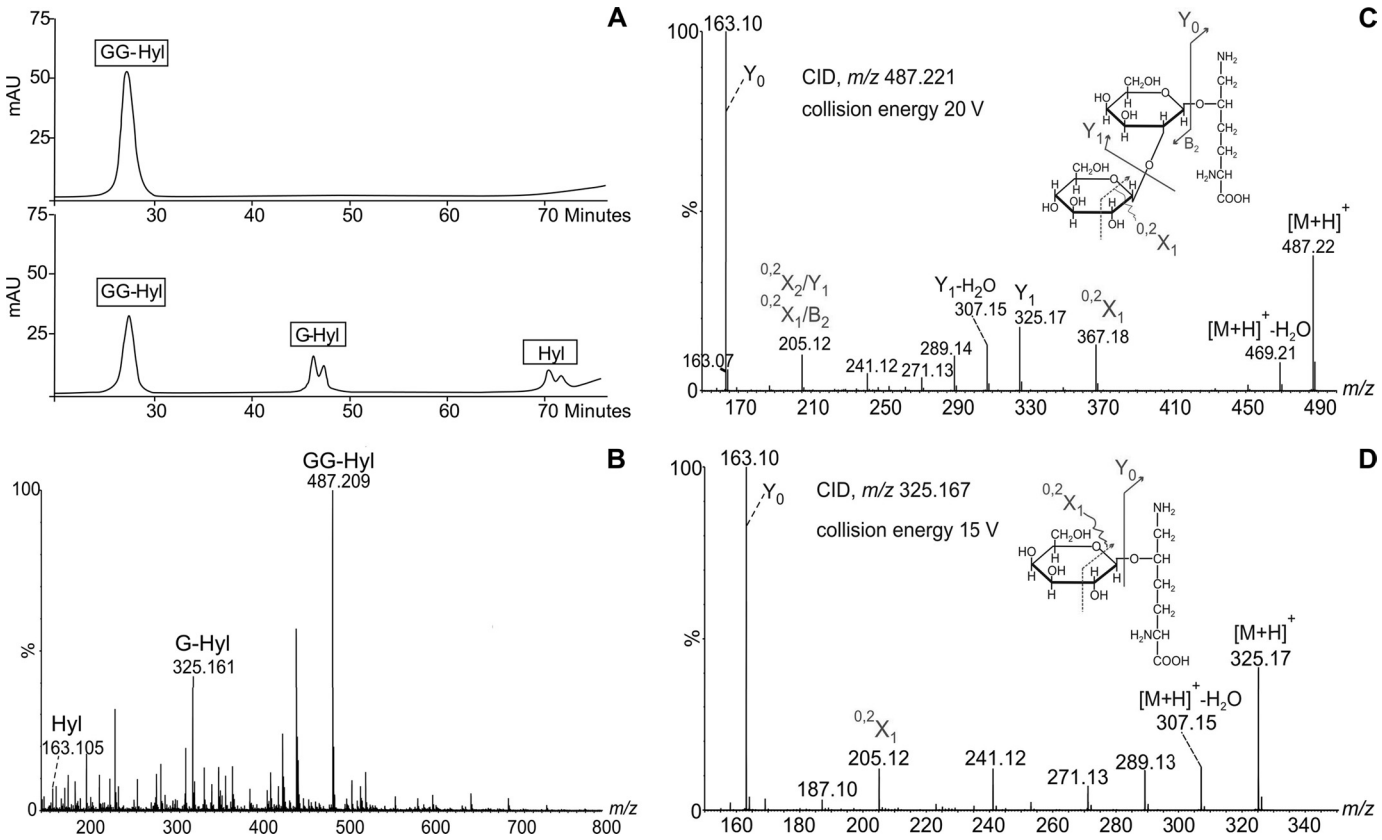

FIGURE 5. **Purification and identification of glycosylated Hyl standards.** *A*, *upper panel*, ion exchange chromatogram of potential GG-Hyl residues isolated from a P-2 column. *Lower panel*, ion exchange chromatogram of the same compound after mild acid hydrolysis, showing the conversion into free Hyl and an intermediate product, potentially G-Hyl. *B*, mass spectrum of the mixture of Hyl, G-Hyl, and GG-Hyl from the amino acid analysis, showing the molecular ions corresponding to each species. *C* and *D*, MS/MS spectra of the ions of *m/z* 487.221 and 325.167, confirming the structures of GG-Hyl and G-Hyl, respectively. *CID*, collision-induced dissociation; *mAU*, milli-absorbance units.

The identity of the purified GG-Hyl residues was indirectly confirmed through the conversion of GG-Hyl into G-Hyl and free Hyl by mild acid hydrolysis. Fig. 5*A*, *upper panel*, shows the chromatogram of the potential GG-Hyl residue separated on a strong cation exchange column and detected by the ninhydrin derivatization method. The program was specifically developed to separate GG-, G-, and free Hyl from one another and from other known amino acids. The *lower panel* shows the same compound after mild acid hydrolysis demonstrating a decrease in the amount of the potential GG-Hyl and the appearance of two additional ninhydrin-positive peaks eluting at later time points. The double peak eluting at ~70 min is consistent with the elution of the Hyl standard. The double peak eluted at ~47 min is most likely the intermediate product in the conversion of GG-Hyl into free Hyl, *i.e.* G-Hyl residue, based on the physicochemical characteristics of the molecule and previous reports (50, 53, 57–58).

To confirm the identity, the mild acid hydrolysate containing a mixture of the potential three Hyl species was analyzed on a QTof Global mass spectrometer by nanoelectrospray ionization. The most abundant ion in the MS spectrum shown in Fig. 5*B*, observed as *m/z* 487.209 (1+), was assigned to hydroxylysine modified with dihexose, GG-Hyl. The ion corresponding to the G-Hyl species was observed as *m/z* 325.161. Unmodified Hyl was observed as the singly protonated ion of *m/z* 163.105. The structural characterization of each compound was performed by MS/MS (shown in Fig. 5, *C* and *D*). The fragment ions observed in the MS/MS spectrum of the ion of *m/z* 487.209 (obtained with a collision energy of 20 V) are characteristic for the collision-induced dissociation spectra of glycoconjugates, confirming the structure GG-Hyl (Fig. 5*C*). The fragment ions of *m/z* 325.165 and 163.103, assigned to Y_1 and Y_0 (59), are derived from the subsequent neutral loss of each hexose from the non-reducing end, whereas the ion of *m/z* 367.178, assigned to $^{0,2}X_1$, resulted from a cross-ring cleavage in the first monosaccharide ring. The ion of *m/z* 205.116 is most likely formed in a secondary fragmentation event by cross-ring cleavage within the Y_1 fragment. This hypothesis is supported by the fact that, by increasing the collision energy, this ion is observed with higher relative abundance. The fragment ions observed in the collision-induced dissociation spectrum of the ion of *m/z* 325.167 (shown in Fig. 5*D*) were obtained using a collision energy of 15 V. The most abundant ion, *m/z* 163.101, Y_0, is derived from the fragmentation of G-Hyl from the non-reducing end.

Quantification of GG-Hyl, G-Hyl, and Free Hyl—To separate and quantify the level of GG-Hyl, G-Hyl, and free Hyl, a new program was developed on the amino acid analysis system in our laboratory by modifying the buffer gradient (Table 1) reported previously (46). The separation of the glycosylated Hyl and the other amino acid standard is shown in Fig. 6. This specific program can be used to analyze base hydrolysates of

TABLE 1

Gradient system used for separation of GG-Hyl, G-Hyl, and free Hyl

Buffer A, 125 mM tartaric acid disodium, 172 mM maleic acid, 2.5% isopropyl alcohol, pH 2.78; Buffer B, 0.3 M NaOH, 107.7 mM maleic acid, 48.5 mM boric acid, pH 9.91.

Minutes	*Buffer A*	*Buffer B*	*Oven Temp.*	*UV Monitor*
Initial	100	0		
1.5	100	0		
3	60	40	60°C	
27	59	41	67 min	
33	43	57		
45	43	57		570nm
46	12	88		
70	12	88	90°C	
85	10	90	43 min	
110	0	100		
120	0	100		

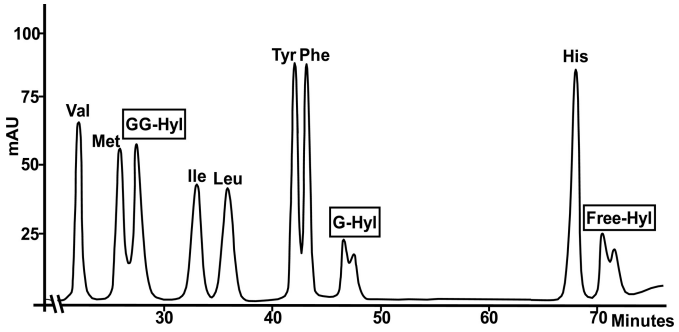

FIGURE 6. **HPLC elution profile of GG-Hyl, G-Hyl, and free Hyl relative to other amino acids.** The *three-letter abbreviations* are used to indicate amino acids. *mAU*, milli-absorbance units.

collagens as the carbohydrate units are retained under these conditions. Fig. 7 shows the levels of the different Hyl species in type I collagen purified from control cells and clones and analyzed in triplicates. The results revealed that there was a significant decrease in the level of GG-Hyl with a concomitant increase in the level of G-Hyl in collagen from Sh clones, whereas the levels of free Hyl remained comparable between the Sh clones and the controls, MC, and EV. This modification profile was also confirmed in type I collagen purified from the other two independent sets of cultures. This clearly indicates that the major role of LH3 for type I collagen in osteoblasts is to transfer glucose units to G-Hyl residues.

Purification of Recombinant LH3-V5/His Fusion Protein—To confirm the glycosyltransferase activity of LH3, recombinant LH3-V5/His fusion protein was purified from the culture medium of 293 HEK cells. An aliquot from the collected fractions was analyzed by a 4–12% NuPAGE Bis-Tris gel stained with CBB and by Western blot analyses (Fig. 8). By CBB staining, a major single band was observed at ~96 kDa consistent with the expected molecular mass of LH3-V5/His fusion protein (91-kDa LH3 + 5-kDa tag). The identity of the purified protein was further confirmed by Western blot analysis with

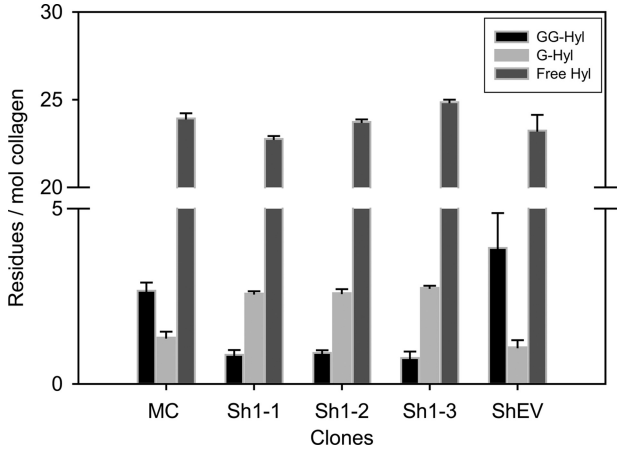

FIGURE 7. **Glycosylation levels of Hyl residues in purified type I collagen synthesized by Sh1 clones and controls.** The levels of GG-Hyl, G-Hyl, and free Hyl are shown as residues/mol of collagen. *Error bars* indicate mean ± S.D. of triplicate analyses of the hydrolysates.

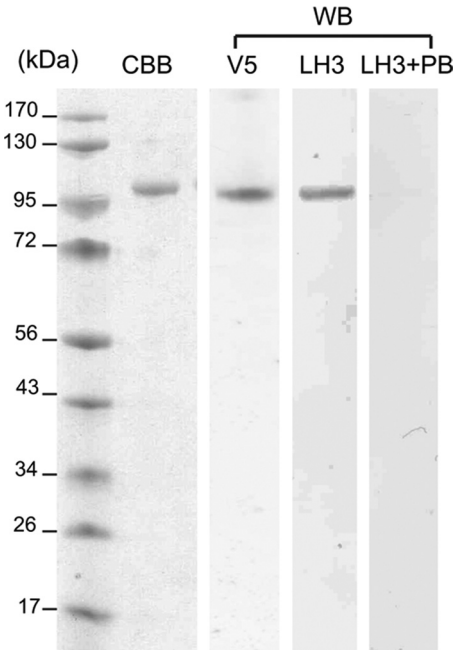

FIGURE 8. **Characterization of recombinant LH3-V5/His-tagged protein.** Purified LH3-V5/His protein was subjected to a 4–12% NuPAGE Bis-Tris gel, staining with CBB, and Western blot (*WB*) analyses with anti-V5 antibody (*V5*), anti-LH3 antibody (*LH3*), and anti-LH3 antibody with a 15-fold molar excess of blocking peptide (*LH3+PB*). The major band at the level of ~96 kDa showed immunoreactivities to both anti-V5 and anti-LH3 antibodies.

anti-V5 and anti-LH3 antibodies. In both cases, a single, immunoreactive ~96-kDa band was observed. When an immunizing peptide blocking experiment was performed, even with a level of 15-fold molar excess of peptide blocking, the immunoreactivity of the protein to anti-LH3 antibody was almost completely abolished, indicating the competitive binding of the peptides to anti-LH3 antibody. With higher concentrations of the peptide, no immunoreactivity of the protein was observed (data not shown). The fractions were then pooled, dialyzed, and concentrated.

Glycosyltransferase Activity of LH3-V5/His Fusion Protein—The results of the GT and GGT activity assays of LH3-V5/His fusion protein with bovine skin collagen substrate are shown in

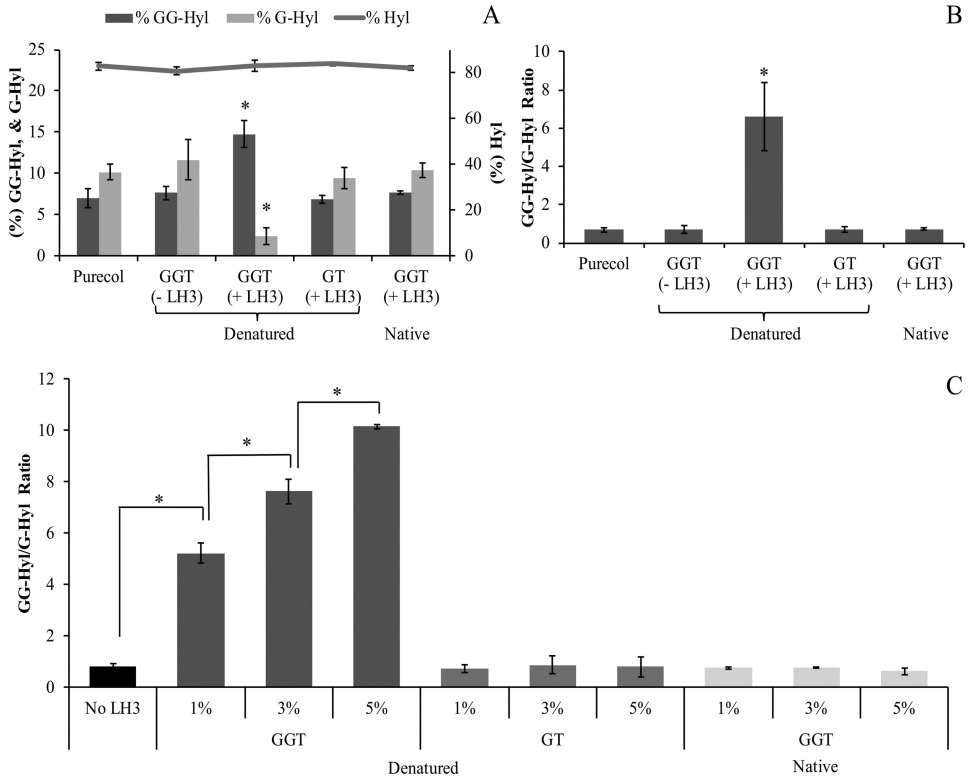

FIGURE 9. **HPLC-based glycosyltransferase activity assays of recombinant LH3-V5/His against denatured and native type I collagen.** The transfer of galactose to Hyl (GT activity) or glucose to galactosyl-Hyl (GGT activity) in type I collagen by recombinant LH3-V5/His protein was performed with denatured and native bovine skin collagen (PureCol) substrate. The levels of free Hyl, G-Hyl, and GG-Hyl in collagen were determined by HPLC as shown in Fig. 6. *A*, percentages of Hyl, G-Hyl, and GG-Hyl of total Hyl in the collagen substrate before (*PureCol*) and after the reaction for GT and GGT activities using LH3-V5/His protein (1% (w/w) of collagen substrate). *, $p < 0.05$ compared with control (PureCol). *B*, GG-Hyl/G-Hyl ratios calculated from *A*. *, $p < 0.05$ compared with control (PureCol). *C*, GG-Hyl/G-Hyl ratios from the GGT and GT activity assays using increasing levels of LH3-V5/His proteins (1, 3, and 5% (w/w) of collagen substrate) with denatured or native collagen substrate. *, $p < 0.05$ between the two groups indicated by a *bracket*. *LH3*, LH3-V5/His protein. *Error bars* indicate mean ± S.D. from each assay done in triplicate. *, significant difference ($p < 0.05$).

Fig. 9. When LH3-V5/His fusion protein was incubated with denatured collagen substrate, the level of GG-Hyl was significantly increased with a concomitant decrease in the level of G-Hyl (Fig. 9*A*), leading to a reverse in the GG-Hyl/G-Hyl ratio (Fig. 9*B*). However, the transfer of galactose units to free Hyl was not observed as the GG-Hyl/G-Hyl ratio did not change (Fig. 9*B*). When native bovine skin collagen was used as a substrate, the GGT activity was not observed (Fig. 9, *A* and *B*). To confirm the specificity of the enzymatic functions, the dose effect of LH3-V5/His protein was examined (Fig. 9*C*). With denatured collagen substrate, the change in the GG-Hyl/G-Hyl ratio and the dose effect were observed only for the GGT activity but not the GT activity. The GGT activity was readily detected with an amount of LH3-V5/His protein as low as 0.1% of the collagen substrate (w/w), indicating a strong potency of the recombinant LH3-V5/His fusion protein as an enzyme (data not shown). When native collagen was used as a substrate, the GG-Hyl/G-Hyl ratio was not changed with any levels of LH3-V5/His protein examined (Fig. 9*C*). Similar results were observed when rat tail tendon collagen was used as a substrate for the GT and GGT activity assays (data not shown). The results shown here indicate that the purified LH3-V5/His protein is enzymatically active with a specific function of glucosylation of G-Hyl residues and suggest that the specific substrates for LH3 are the collagen α chains rather than the native collagen molecules, which is consistent with previous reports showing that the triple helical conformation of collagens inhibited further post-translational modifications (60, 61).

DISCUSSION

During the past decade, several reports have shown the unique features of LH3, *i.e.* its multifunctionality (LH, GT, and GGT activities) (25–27, 62) and its intra- as well as extracellular localization (55). The critical importance of this enzyme for connective tissue integrity was clearly demonstrated through the gene knock-out mouse study and others (29, 30, 32, 33). The enzymatic functions of LH3 were shown through *in vitro* activity assays using lysates from SF9 cells transfected with LH3 expression plasmid, cell-free translation, or purified recombinant LH3 protein as the enzyme source (25–27, 62). The GGT activity of LH3 and its biological significance have been well demonstrated; however, data regarding the GT activity of LH3 have been somewhat conflicting (25, 27, 28). Recently, Schegg *et al.* (34) have reported the cloning of novel collagen galactosyltransferase enzymes GLT25D1 and GLT25D2 and showed that these enzymes were capable of transferring galactose units to free Hyl residues in collagen, whereas LH3 was not. However, direct measurements of the amount of G-Hyl or GG-Hyl residues were rarely performed in the assays used in the past. In this study, we successfully purified the G-Hyl and

GG-Hyl standards from natural marine sponge and developed a specific HPLC program that allowed us to effectively separate and quantify the levels of GG-Hyl, G-Hyl, and free Hyl residues in the base hydrolysate of the collagen samples.

Type I collagen is the major collagen type in most connective tissues, including skin, bone and tendon. However, little is known about the role of LH3 in this major fibrillar collagen at present. In this study, by using the short hairpin RNA technique in mouse osteoblasts, we successfully generated single cell-derived clones stably suppressing LH3 and characterized its effect on type I collagen post-translational modifications. Our data demonstrated that the major function of LH3 is to glucosylate G-Hyl residues in type I collagen. The simultaneous increase in the level of G-Hyl residues observed from the LH3 Sh clones is most likely the result of a diminished level of glucose transfer by LH3 suppression. The gene expression of GLT25D1, another potential galactosyltransferase, was unaffected by LH3 suppression. In addition, the levels of free and total Hyl residues in the purified type I collagen were essentially unchanged among the Sh clones and controls, suggesting that the LH activity of LH3, if any, is minimal for bone type I collagen. In the past years, several groups have tried to determine the sequence or collagen type specificity for the activities of LH isoforms (28, 29, 63–70). The results from these studies indicated that there are no strict collagen types or sequence requirements for the individual LH isoforms. It was suggested that LH2b, the major isoform of LH2 in bone, mainly hydroxylates Lys residues in the telopeptide regions, thus determining the collagen cross-linking pathway (65, 67, 71–73). In contrast, LH1 preferentially catalyzes the hydroxylation of Lys residues in the triple helical region of fibrillar collagen, including those residues pairing with the telopeptidyl Hyl/Lys aldehydes to form the intermolecular cross-links (29, 65, 66, 68, 74). As for LH3, its contribution to Lys hydroxylation in the helical region of fibrillar collagen is still unclear (28, 29, 65). When the function of one isoform is impaired, compensatory mechanisms from the other two isoforms may occur and may depend largely on the tissue-specific expression of each isoform (70).

In this study, the enzymatic function of LH3 as the main GGT but not GT was also confirmed by using the enzymatically active recombinant mouse LH3-V5/His fusion protein generated by 293 HEK cells culture. By using HPLC, we could directly measure the levels of GG-Hyl and G-Hyl in the reaction products of the GGT and GT activity assays. The specificity of the glucosylation activity of LH3-V5/His protein against denatured type I collagen was demonstrated by the dose -dependent increase of GG-Hyl when increasing amounts of LH3-V5/His protein were used. Furthermore, no transfer of galactose was observed even with increasing amounts of LH3-V5 protein. This result is consistent with studies showing that the GT activity of LH3 protein is very low (25, 27) or even undetectable (28, 34) in contrast to the GGT activity. As for the expressions of *Glt25d1* and *-2*, only the former isoform was detected in MC cells. From our results and those recently reported by Schegg *et al.* (34), it is likely that galactosylation of Hyl in bone type I collagen is catalyzed by protein followed by subsequent glucosylation by LH3.

The ability of recombinant LH3 to modify extracellular proteins (collagen or other proteins) as shown by the GGT activity assay indicated that LH3, unlike LH1 and LH2, is localized and functional in the extracellular space as well (55). However, the specific substrates for the extracellular function of LH3, such as collagens or proteins with collagenous sequences, have never been identified but were assumed to be collagen. Interestingly, this finding contradicts with the earlier reports that triple helical conformation inhibits further modifications (60, 61). Thus, it was proposed that at physiological temperature there is a possibility of micro-unfolding of the triple helix, which allows further modifications (55). In our study, when native bovine skin collagen was used as a substrate for the GGT activity assay, an increase in the level of GG-Hyl was not observed as seen with denatured collagen substrate. This finding could suggest that the specific substrate for the enzymatic function of extracellular LH3 may not be type I collagen or that the secreted LH3 may play a different role.

From the current study, it is apparent that a decrease in glucosylation of G-Hyl in type I collagen significantly affects the collagen fibril formation kinetics observed in the *in vitro* fibrillogenesis assay. The collagen molecules with less glucosylation could self-aggregate faster and form thicker fibrils due in part to lesser steric hindrance for the molecular packing. This result is consistent with other reports showing that the degree of collagen modification is inversely correlated to the rate and diameter size of collagen fibrils formed *in vitro* (3, 7, 75).

It has been shown that one of the major cross-linking sites in the helical region of type I collagen (residue 87 of α1 and α2 chains) is mainly diglycosylated (8–10, 76–79). Thus, further studies are warranted to investigate the potential effects of the pattern (di- *versus* monoglycosylation) and extent of glycosylation on cross-link formation and maturation.

Taken together, the results of this study show that, by manipulating the LH3 gene expression in mouse osteoblasts, the major function of LH3 is to transfer glucose units to G-Hyl residues in the α chains of bone type I collagen. This result was also corroborated with the HPLC-based glycosyltransferase activity assays using recombinant LH3-V5/His fusion protein. The significant decrease in the transfer of glucose units, through LH3 suppression, results in the change in the *in vitro* collagen fibril formation kinetics. It can be concluded that the levels and types of Hyl glycosylation and possibly its loci in type I collagen are indeed critical for proper formation of collagen fibrils.

Acknowledgments—We thank Dr. Yoshiyuki Mochida (Boston University) for valuable suggestions during the course of the study and Dr. Franck Polleux (Neuroscience Center, University of North Carolina at Chapel Hill) for providing us with the pSilencer2.1 vector for the preliminary experiments.

REFERENCES

1. Gordon, M. K., and Hahn, R. A. (2010) *Cell Tissue Res.* **339,** 247–257
2. Carter, E. M., and Raggio, C. L. (2009) *Curr. Opin. Pediatr.* **21,** 46–54
3. Amudeswari, S., Liang, J. N., and Chakrabarti, B. (1987) *Coll. Relat. Res.* **7,** 215–223
4. Bätge, B., Winter, C., Notbohm, H., Acil, Y., Brinckmann, J., and Müller,

P. K. (1997) *J. Biochem.* **122,** 109–115
5. Notbohm, H., Nokelainen, M., Myllyharju, J., Fietzek, P. P., Müller, P. K., and Kivirikko, K. I. (1999) *J. Biol. Chem.* **274,** 8988–8992
6. Torre-Blanco, A., Adachi, E., Hojima, Y., Wootton, J. A., Minor, R. R., and Prockop, D. J. (1992) *J. Biol. Chem.* **267,** 2650–2655
7. Yang, C. L., Rui, H., Mosler, S., Notbohm, H., Sawaryn, A., and Müller, P. K. (1993) *Eur. J. Biochem.* **213,** 1297–1302
8. Henkel, W., Rauterberg, J., and Stirtz, T. (1976) *Eur. J. Biochem.* **69,** 223–231
9. Eyre, D. R., and Glimcher, M. J. (1973) *Biochem. Biophys. Res. Commun.* **52,** 663–671
10. Eyre, D. R., and Glimcher, M. J. (1973) *Biochem. J.* **135,** 393–403
11. Hanson, D. A., and Eyre, D. R. (1996) *J. Biol. Chem.* **271,** 26508–26516
12. Robins, S. P. (1983) *Biochem. J.* **215,** 167–173
13. Gineyts, E., Garnero, P., and Delmas, P. D. (2001) *Rheumatology* **40,** 315–323
14. Moro, L., Romanello, M., Favia, A., Lamanna, M. P., and Lozupone, E. (2000) *Calcif. Tissue Int.* **66,** 151–156
15. Cunningham, L. W., Ford, J. D., and Segrest, J. P. (1967) *J. Biol. Chem.* **242,** 2570–2571
16. Segrest, J. P., and Cunningham, L. W. (1970) *J. Clin. Investig.* **49,** 1497–1509
17. Rauch, F., Schnabel, D., Seibel, M. J., Remer, T., Stabrey, A., Michalk, D., and Schönau, E. (1995) *J. Clin. Endocrinol. Metab.* **80,** 1295–1300
18. Al-Dehaimi, A. W., Blumsohn, A., and Eastell, R. (1999) *Clin. Chem.* **45,** 676–681
19. Moro, L., Noris-Suarez, K., Michalsky, M., Romanello, M., and de Bernard, B. (1993) *Biochim. Biophys. Acta* **1156,** 288–290
20. Michalsky, M., Stepan, J. J., Wilczek, H., Formankova, J., and Moro, L. (1995) *Clin. Chim. Acta* **234,** 101–108
21. Bettica, P., Taylor, A. K., Talbot, J., Moro, L., Talamini, R., and Baylink, D. J. (1996) *J. Clin. Endocrinol. Metab.* **81,** 542–546
22. Pecile, A., Netti, C., Sibilia, V., Villa, I., Calori, G., Tenni, R., Coluzzi, M., Moro, G. L., and Rubinacci, A. (1996) *J. Endocrinol.* **150,** 383–390
23. Vogel, W., Gish, G. D., Alves, F., and Pawson, T. (1997) *Mol. Cell* **1,** 13–23
24. Myers, L. K., Myllyharju, J., Nokelainen, M., Brand, D. D., Cremer, M. A., Stuart, J. M., Bodo, M., Kivirikko, K. I., and Kang, A. H. (2004) *J. Immunol.* **172,** 2970–2975
25. Heikkinen, J., Risteli, M., Wang, C., Latvala, J., Rossi, M., Valtavaara, M., and Myllylä, R. (2000) *J. Biol. Chem.* **275,** 36158–36163
26. Wang, C., Risteli, M., Heikkinen, J., Hussa, A. K., Uitto, L., and Myllyla, R. (2002) *J. Biol. Chem.* **277,** 18568–18573
27. Wang, C., Luosujärvi, H., Heikkinen, J., Risteli, M., Uitto, L., and Myllylä, R. (2002) *Matrix Biol.* **21,** 559–566
28. Rautavuoma, K., Takaluoma, K., Sormunen, R., Myllyharju, J., Kivirikko, K. I., and Soininen, R. (2004) *Proc. Natl. Acad. Sci. U.S.A.* **101,** 14120–14125
29. Ruotsalainen, H., Sipilä, L., Vapola, M., Sormunen, R., Salo, A. M., Uitto, L., Mercer, D. K., Robins, S. P., Risteli, M., Aszodi, A., Fässler, R., and Myllylä, R. (2006) *J. Cell Sci.* **119,** 625–635
30. Sipilä, L., Ruotsalainen, H., Sormunen, R., Baker, N. L., Lamandé, S. R., Vapola, M., Wang, C., Sado, Y., Aszodi, A., and Myllylä, R. (2007) *J. Biol. Chem.* **282,** 33381–33388
31. Savolainen, E. R., Kero, M., Pihlajaniemi, T., and Kivirikko, K. I. (1981) *N. Engl. J. Med.* **304,** 197–204
32. Risteli, M., Ruotsalainen, H., Salo, A. M., Sormunen, R., Sipilä, L., Baker, N. L., Lamandé, S. R., Vimpari-Kauppinen, L., and Myllylä, R. (2009) *J. Biol. Chem.* **284,** 28204–28211
33. Salo, A. M., Cox, H., Farndon, P., Moss, C., Grindulis, H., Risteli, M., Robins, S. P., and Myllylä, R. (2008) *Am. J. Hum. Genet.* **83,** 495–503
34. Schegg, B., Hülsmeier, A. J., Rutschmann, C., Maag, C., and Hennet, T. (2009) *Mol. Cell Biol.* **29,** 943–952
35. Cetta, G., De Luca, G., Tenni, R., Zanaboni, G., Lenzi, L., and Castellani, A. A. (1983) *Connect Tissue Res.* **11,** 103–111
36. Tenni, R., Valli, M., Rossi, A., and Cetta, G. (1993) *Am. J. Med. Genet.* **45,** 252–256
37. Bateman, J. F., Mascara, T., Chan, D., and Cole, W. G. (1984) *Biochem. J.* **217,** 103–115
38. Moro, L., Bettica, P., Romanello, M., and Suarez, K. N. (1997) *Eur. J. Clin. Chem. Clin. Biochem.* **35,** 29–33
39. Moro, L., Suarez, K. N., and Romanello, M. (1997) *Eur. J. Clin. Chem. Clin. Biochem.* **35,** 269–273
40. Michalsky, M., Norris-Suarez, K., Bettica, P., Pecile, A., and Moro, L. (1993) *Biochem. Biophys. Res. Commun.* **192,** 1281–1288
41. Dominguez, L. J., Barbagallo, M., and Moro, L. (2005) *Biochem. Biophys. Res. Commun.* **330,** 1–4
42. Lehmann, H. W., Wolf, E., Röser, K., Bodo, M., Delling, G., and Müller, P. K. (1995) *J. Cancer Res. Clin. Oncol.* **121,** 413–418
43. Wang, D., Christensen, K., Chawla, K., Xiao, G., Krebsbach, P. H., and Franceschi, R. T. (1999) *J. Bone Miner. Res.* **14,** 893–903
44. Livak, K. J., and Schmittgen, T. D. (2001) *Methods* **25,** 402–408
45. Parisuthiman, D., Mochida, Y., Duarte, W. R., and Yamauchi, M. (2005) *J. Bone Miner. Res.* **20,** 1878–1886
46. Yamauchi, M., and Shiiba, M. (2008) *Methods Mol. Biol.* **446,** 95–108
47. Vogel, K. G., Paulsson, M., and Heinegård, D. (1984) *Biochem. J.* **223,** 587–597
48. Williams, B. R., Gelman, R. A., Poppke, D. C., and Piez, K. A. (1978) *J. Biol. Chem.* **253,** 6578–6585
49. Tenni, R., Rimoldi, D., Zanaboni, G., Cetta, G., and Castellani, A. A. (1984) *Ital. J. Biochem.* **33,** 117–127
50. Garza, H., Bennett, N., Jr., and Rodriguez, G. P. (1996) *J. Chromatogr. A* **732,** 385–389
51. Yamauchi, M., London, R. E., Guenat, C., Hashimoto, F., and Mechanic, G. L. (1987) *J. Biol. Chem.* **262,** 11428–11434
52. Cetta, G., Tenni, R., Zanaboni, G., De Luca, G., Ippolito, E., De Martino, C., and Castellani, A. A. (1982) *Biochem. J.* **204,** 61–67
53. Askenasi, R. (1973) *Biochim. Biophys. Acta* **304,** 375–383
54. Lou, M. F., and Hamilton, P. B. (1971) *Clin. Chem.* **17,** 782–788
55. Salo, A. M., Wang, C., Sipilä, L., Sormunen, R., Vapola, M., Kervinen, P., Ruotsalainen, H., Heikkinen, J., and Myllylä, R. (2006) *J. Cell Physiol.* **207,** 644–653
56. Wood, G. C., and Keech, M. K. (1960) *Biochem. J.* **75,** 588–598
57. Odell, V., Wegener, L., Peczon, B., and Hudson, B. G. (1974) *J. Chromatogr.* **88,** 245–252
58. Peczon, B. D., Antreasian, R., and Bucay, P. (1979) *J. Chromatogr.* **169,** 351–356
59. Domon, B., and Costello, C. E. (1988) *Glycoconj. J.* **5,** 397–409
60. Myllylä, R., Risteli, L., and Kivirikko, K. I. (1975) *Eur. J. Biochem.* **58,** 517–521
61. Oikarinen, A., Anttinen, H., and Kivirikko, K. I. (1977) *Biochem. J.* **166,** 357–362
62. Rautavuoma, K., Takaluoma, K., Passoja, K., Pirskanen, A., Kvist, A. P., Kivirikko, K. I., and Myllyharju, J. (2002) *J. Biol. Chem.* **277,** 23084–23091
63. Risteli, M., Niemitalo, O., Lankinen, H., Juffer, A. H., and Myllylä, R. (2004) *J. Biol. Chem.* **279,** 37535–37543
64. Wang, C., Valtavaara, M., and Myllylä, R. (2000) *DNA Cell Biol.* **19,** 71–77
65. Takaluoma, K., Lantto, J., and Myllyharju, J. (2007) *Matrix Biol.* **26,** 396–403
66. Uzawa, K., Yeowell, H. N., Yamamoto, K., Mochida, Y., Tanzawa, H., and Yamauchi, M. (2003) *Biochem. Biophys. Res. Commun.* **305,** 484–487
67. Pornprasertsuk, S., Duarte, W. R., Mochida, Y., and Yamauchi, M. (2004) *J. Bone Miner. Res.* **19,** 1349–1355
68. Zuurmond, A. M., van der Slot-Verhoeven, A. J., van Dura, E. A., De Groot, J., and Bank, R. A. (2005) *Matrix Biol.* **24,** 261–270
69. Bank, R. A., Robins, S. P., Wijmenga, C., Breslau-Siderius, L. J., Bardoel, A. F., van der Sluijs, H. A., Pruijs, H. E., and TeKoppele, J. M. (1999) *Proc. Natl. Acad. Sci. U.S.A.* **96,** 1054–1058
70. Takaluoma, K., Hyry, M., Lantto, J., Sormunen, R., Bank, R. A., Kivirikko, K. I., Myllyharju, J., and Soininen, R. (2007) *J. Biol. Chem.* **282,** 6588–6596
71. Uzawa, K., Grzesik, W. J., Nishiura, T., Kuznetsov, S. A., Robey, P. G., Brenner, D. A., and Yamauchi, M. (1999) *J. Bone Miner. Res.* **14,** 1272–1280
72. Mercer, D. K., Nicol, P. F., Kimbembe, C., and Robins, S. P. (2003) *Biochem. Biophys. Res. Commun.* **307,** 803–809
73. van der Slot, A. J., Zuurmond, A. M., Bardoel, A. F., Wijmenga, C., Pruijs,

H. E., Sillence, D. O., Brinckmann, J., Abraham, D. J., Black, C. M., Verzijl, N., DeGroot, J., Hanemaaijer, R., TeKoppele, J. M., Huizinga, T. W., and Bank, R. A. (2003) *J. Biol. Chem.* **278,** 40967–40972
74. Eyre, D., Shao, P., Weis, M. A., and Steinmann, B. (2002) *Mol. Genet. Metab.* **76,** 211–216
75. Guitton, J. D., Le Pape, A., Sizaret, P. Y., and Muh, J. P. (1981) *Biosci. Rep.* **1,** 945–954
76. Butler, W. T., and Cunningham, L. W. (1966) *J. Biol. Chem.* **241,** 3882–3888
77. Cunningham, L. W., and Ford, J. D. (1968) *J. Biol. Chem.* **243,** 2390–2398
78. Morgan, P. H., Jacobs, H. G., Segrest, J. P., and Cunningham, L. W. (1970) *J. Biol. Chem.* **245,** 5042–5048
79. Aguilar, J. H., Jacobs, H. G., Butler, W. T., and Cunningham, L. W. (1973) *J. Biol. Chem.* **248,** 5106–5113